FULL PAPER

Dalton
www.rsc.org/dalton

Synthesis, characterization and reactivity of heterobimetallic complexes (η^5-C_5R_5)Ru(CO)(μ-dppm)M(CO)$_2$(η^5-C_5H_5) (R = H, CH_3; M = Mo, W). Interconversion of hydrogen/carbon dioxide and formic acid by these complexes†

Man Lok Man, Zhongyuan Zhou, Siu Man Ng and Chak Po Lau*

Department of Applied Biology and Chemical Technology, The Hong Kong Polytechnic University, Hung Hom, Kowloon, Hong Kong, China.
E-mail: bccplau@polyu.edu.hk; Fax: 852-23649932; Tel: 852-27665619

Received 16th June 2003, Accepted 14th August 2003
First published as an Advance Article on the web 26th August 2003

The heterobimetallic complexes [(η^5-C_5R_5)Ru(CO)(μ-dppm)M(CO)$_2$(η^5-C_5H_5)] (M = Mo, W; R = H, CH_3) (**1**–**4**) are prepared by metathetical reactions between (η^5-C_5R_5)Ru(dppm)Cl and $Na^+[(\eta^5\text{-}C_5H_5)M(CO)_3]^-$. IR spectroscopic and X-ray structural studies show that each of these complexes contains a semi-bridging carbonyl ligand. The low activity of these complexes in catalytic CO_2 hydrogenation to formic acid might be attributed to their non-facile reactions with H_2 to yield the active dihydride species. The metal–metal bonds can be protonated to form the cationic complexes, which contain strong Ru–H–M bridges. The bridging hydrogen atom is weakly acidic since it can be removed by a strong base, and it protonates BPh_4^- to give BPh_3 and benzene. It also reacts with the hydridic hydrogen of Et_3SiH to yield H_2. The bridging hydrogen, however, cannot be removed by hydride scavengers such as $Ph_3C^+OTf^-$ and $Me_3Si^+OTf^-$. The sluggishness of the catalytic formic acid decomposition by **1**–**4** is attributable to the stability of the protonated bimetallic intermediate [(η^5-C_5R_5)Ru(CO)(μ-dppm)(μ-H)M(CO)$_2$(η^5-C_5H_5)]$^+HCOO^-$ formed during the catalysis.

Introduction

The unconventional hydrogen bond (dihydrogen bond) between a transition metal hydride and a common hydrogen bond donor containing an O–H or an N–H group is a hydride–proton interaction. Complexes containing this H ⋯ H interaction of the type M–H ⋯ H–O or M–H ⋯ H–N might be regarded as intermediates in hydride protonation to generate a η^2-H_2 ligand and the reverse reaction, *i.e.*, heterolytic splitting of dihydrogen. The dihydrogen bond is also recognized for activating the M–H bond for reactions such as H/D exchanges, proton transfer, and substitution.[1] It is also well-demonstrated that the dihydrogen bond plays an important role in controlling the reactivity and stereochemistry of organometallic hydride complexes.[2]

We have synthesized and characterized intramolecular Ru–H ⋯ H–N dihydrogen-bonding in aminocyclopentadienyl ruthenium hydride complexes and have also demonstrated that the Ru–H ⋯ H–N dihydrogen bond is a key feature in the catalytic hydrogenation of CO_2 to formic acid.[3] We envision that replacing the N–H function with a metal fragment M–H, which is relatively less hydridic, might generate bimetallic systems containing a Ru–H ⋯ H–M dihydrogen bond, these systems might exhibit interesting reactivity.

Bimetallic complexes have attracted considerable interest because they have the potential of giving unique chemistry, and are promising candidates for new chemical reactions and catalysis.[4] The proximity of the metal centers offers the possibility of cooperative reactivity – the metal centers operating in concert, with reactivity of the individual metal atoms complementing each other.[5] It was reported that the unsymmetrical metal–metal bond in the early–late heterobimetallic complex $Cp_2Zr(\mu\text{-}N^tBu)IrCp^*$ was cleaved by H_2 to form the hydride complex $Cp_2Zr(H)(\mu\text{-}H)(\mu\text{-}N^tBu)IrCp^*$; CO_2 insertion into the terminal hydride gave two diastereomeric heterobimetallic formato complexes $Cp_2Zr(OC(O)H)(\mu\text{-}H)(\mu\text{-}N^tBu)IrCp^*$, which could be converted stoichiometrically to formic acid.[6] More recently, Puddephatt and co-workers have demonstrated that the bimetallic complex [$Ru_2(\mu\text{-}CO)(CO)_4(\mu\text{-}dppm)_2$] has considerably higher activity in catalytic reversible reaction of formic acid to CO_2 and H_2 than the comparable mononuclear ruthenium complex catalysts. The relatively high activity might be related to facile generation of coordination unsaturation in the binuclear system. This is the first binuclear homogeneous catalyst that is reported to directly involve in either the decomposition of formic acid or the hydrogenation of CO_2 to formic acid.[7]

In our attempt to construct the dihydrogen-bonded bimetallic systems, we synthesized, characterized, and studied the reactivity of some Ru–M (M = Mo, W) bimetallic complexes; the catalysis of the reversible reaction of formic acid to carbon dioxide and hydrogen with these complexes was also investigated.

Results and discussion

Syntheses and characterizations of bimetallic complexes 1–4

The Ru–Mo and Ru–W bimetallic complexes were prepared by reacting the ruthenium chloro complex with the sodium salt of the cyclopentadienyl molybdenum or tungsten carbonyl anion (eqn. (1)).

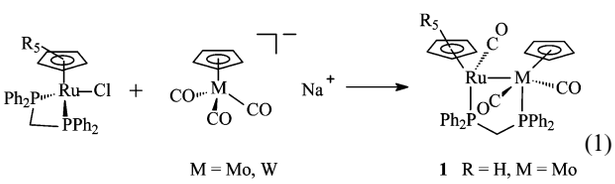

M = Mo, W
R = H, CH_3

(1)

1 R = H, M = Mo
2 R = CH_3, M = Mo
3 R = H, M = W
4 R = CH_3, M = W

† Electronic supplementary information (ESI) available: Selected bond lengths and angles and ORTEP diagrams for complexes **2**–**4** and **6·Cl** and discussion on the structure of **6·Cl**. See http://www.rsc.org/suppdata/dt/b3/b306835h/

DOI: 10.1039/b306835h

Similar metathetical reactions have been employed to prepare bimetallic complexes containing metal–metal bonds.[8] It was reported that a similar heterobimetallic complex **A** formed by reaction of $Li^+[\eta^5\text{-}C_5H_4P(C_6H_4\text{-}p\text{-}CH_3)_2]Mo(CO)_3^-$ with $\{[(C_6H_4\text{-}p\text{-}CH_3)PCH_2]_2RhCl\}_2$ contains a highly polarized $^{\delta+}Rh\text{–}Mo^{\delta-}$ bond; changing the donating phosphine ligands on Rh to carbonyls led to reduction of the metal–metal bond polarity.[9]

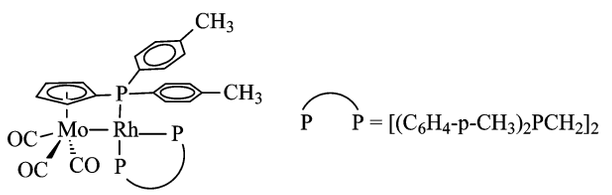

A

The $^{31}P\{^1H\}$ NMR spectrum of each of the complexes **1**–**4** shows a pair of doublets for the dppm ligand. For **1** at δ 49.9 and 53.7 ppm (^2J(PP) = 75.6 Hz); for **2** at δ 46.9 and 58.9 ppm (^2J(PP) = 76.1 Hz); for **3** at δ 21.1 and 56.1 ppm (^2J(PP) = 74.3 Hz); for **4** at δ 21.3 and 48.2 ppm (^2J(PP) = 72.9 Hz). The methylene hydrogen atoms of the dppm ligand of each complex are diastereotopic, they appear as a pair of multiplets. For **1** at δ 3.85 and 4.50 ppm; for **2** at δ 2.87 and 3.67 ppm; for **3** at δ 4.21 and 4.55 ppm; for **4** at δ 2.88 and 3.66 ppm. Each complex shows three carbonyl peaks in the ^{13}C NMR spectrum: for **1**, at δ 249.7 (d, ^2J(PC) = 23.2 Hz), 238.4 (s), and 214.5 ppm (d, ^2J(PC) = 21.0 Hz); for **2**, at δ 252.3 (d, ^2J(PC) = 24.1 Hz), 251.3 (s), and 229.6 ppm (d, ^2J(PC) = 15.5 Hz); for **3**, at δ 238.0 (d, ^2J(PC) = 16.8 Hz), 226.5 (d, ^2J(PC) = 7.4 Hz), and 212.7 ppm (d, ^2J(PC) = 21.2 Hz); for **4**, at δ 239.7 (d, ^2J(PC) = 15.6 Hz), 227.4 (d, ^2J(PC) = 7.4 Hz), and 218.5 ppm (d, ^2J(PC) = 19.9 Hz). The most downfield signal in each case is probably due to the semi-bridging carbonyl (*vide infra*). The carbonyl signals of all four complexes are sharp at room temperature, indicating that there is no scrambling of the carbonyl ligands. IR spectroscopy provides more information about the structures of the complexes. It is observed that in the KBr IR spectrum of each of the complexes **1**–**4**, in addition to the bands due to terminal carbonyl groups, a relatively low energy CO stretching frequency is also present (**1**: 1791 cm^{-1}; **2**: 1777 cm^{-1}; **3**: 1792 cm^{-1}; **4**: 1784 cm^{-1}). The presence of the lower CO stretching frequencies indicates that bridging or semi-bridging carbonyl groups are present in the bimetallic complexes. Moreover, the solution spectra of the complexes in CH_2Cl_2 and THF are basically identical to the KBr spectra, indicative of the perseverance of the bridging or semi-bridging carbonyl groups of **1**–**4** in solution. Semi-bridging carbonyls are not uncommon in bimetallic complexes. For example, the X-ray structures and solid-state IR spectroscopy show that the bimetallic complexes $MoRu(CO)_6(dppm)_2$ [10] and $[RhIr(CH_3)(CO)_2(dppm)_2]^+$ [11] contain semi-bridging carbonyl groups. However, in solutions, the structures of these complexes are somewhat different than in the solid state; the solution IR spectra of these complexes show no CO stretches assignable to semi-bridging carbonyl groups. On the other hand, a semi-bridging carbonyl group was shown by IR spectroscopy to be present in $[MoRh(CO)_4(dppm)(CN^tBu)]Cl$, both in the solid and in solution.[12]

Structures of complexes 1–4

The structures of **1**–**4** have been determined by X-ray crystallography in order to establish whether the carbonyl groups that correspond to the low stretches in IR spectroscopy have bridging or semi-bridging geometry. The molecular structure of the complex **1** is shown in Fig. 1.

Crystal data and refinement details are given in Table 1. Selected bond distances and angles are given in Table 2. (The

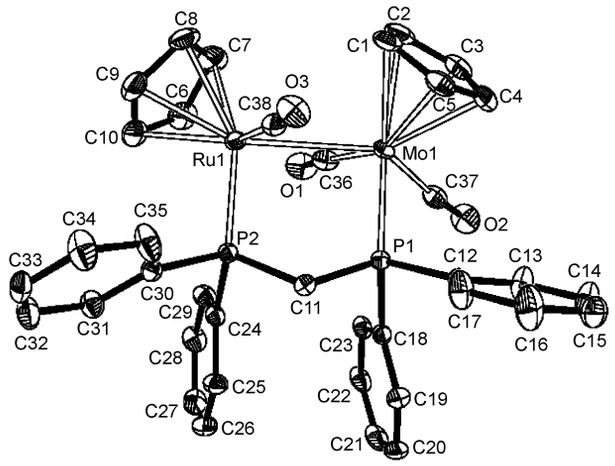

Fig. 1 Molecular structure of CpRu(CO)(μ-dppm)Mo(CO)$_2$Cp (**1**).

molecular structures, crystal data and refinement details, selected bond distances and angles of complexes **2**–**4** can be found in ESI.† The bimetallic complexes are isostructural. In each complex, the ruthenium fragment can be considered as a three-legged piano stool, and the other metal fragment exhibits a four-legged piano-stool geometry. A carbonyl ligand is co-ordinated to the ruthenium center, while two CO groups are bonded to the other metal center. The metal–metal distances of 3.0277(6) and 3.0693(4) Å, respectively, in **1** and **2**, are quite long but do not rule out the presence of metal–metal bonds. A Ru–Mo bond distance of 3.058(1) Å was reported for the heterobimetallic complex $[RuMo(CO)_6(dppm)_2]$.[10] In a recently reported structure of a cluster containing metal–metal bonds linking high-valent molybdenum and low-valent ruthenium centers, one of the ruthenium–molybdenum bonds in the cluster, which is dative in origin (Ru⟶Mo), has a Ru–Mo bond distance of 3.1094(8) Å.[13] We therefore infer the existence of ruthenium–molybdenum metal–metal bonds in **1** and **2**. Similarly, the metal–metal bonds are believed to be present in the isostructural ruthenium–tungsten complexes. The metal–metal distances in **3** and **4** are respectively, 3.0246(11) and 3.0695(4) Å. It is noticeable that in each of the complexes **1**–**4**, the M–C–O (M = Mo, W) angle of the carbonyl ligand, which is closer to the ruthenium center [in **1**, Mo(1)–C(36)–O(1) 168.9(3)°], deviates more from linearity than the M–C–O angle of the other CO ligand on M. Moreover, the distances of the carbon atoms of the less linear carbonyl ligands on M from the ruthenium centers in **1**–**4** fall in the range 2.744–2.906 Å, indicative of weak interaction between these CO ligands and the ruthenium centers. In a Zr–Ru bimetallic complex, the zirconium-bound CO is bent slightly away from the Ru (Zr–C–O 167°) indicating weak interaction with the ruthenium center, which is 2.70 Å from the carbon atom of the carbonyl ligand.[14] One of the iridium bound carbonyls in the bimetallic complex $[RhIr(CO)_3(dppm)_2]$ is semi-bridging; the Ir–C–O (171.9(6)°) deviates significantly from linearity, and the Rh–C distance is 2.644(7) Å.[15]

The carbonyl ligand on M, which interacts with the ruthenium center, can be regarded as semi-bridging CO group. In this bonding mode, the CO accepts electron in its π* orbital from the ruthenium center, which in turn draws electron from M (Chart 1). This semi-bridging bonding mode was studied theoretically by Sargent and Hall.[16] The presence of semi-bridging CO group accounts for the low wavenumber CO stretches in **1**–**4**.

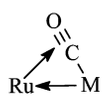

Chart 1

Table 1 Crystal data and refinement details for **1**–**4**, **5·BF$_4$** and **6·Cl** (Bruker Smart 1000CCD diffractometer, refinement method full-matrix least-squares on F^2)

	1	**2**	**3**	**4**	**5·BF$_4$**	**6·Cl**
Empirical forumla	$RuMoC_{38}H_{32}O_3P_2$	$RuMoC_{43}H_{37}O_3P_2.C_2H_5OC_2H_5$	$RuWC_{38}H_{32}O_3P_2$	$RuWC_{43}H_{37}O_3P_2.C_2H_5OC_2H_5$	$C_{38}H_{33}BF_4O_3P_2RuMo$	$C_{40}H_{37}Cl_5O_3P_2RuW$
M_r	795.59	939.84	883.50	1027.75	883.40	1089.81
T/K	294(2)	294(2)	294(2)	294(2)	294(2)	294(2)
λ/Å	0.71073	0.71073	0.71073	0.71073	0.71073	0.71073
Crystal system	Monoclinic	Monoclinic	Monoclinic	Monoclinic	Monoclinic	Monoclinic
Space group	$C2/c$	$P2_1/n$	$C2/c$	$P2_1/n$	Cc	$P2_1/c$
Unit cell dimensions						
a/Å	15.198(3)	13.2833(19)	15.181(8)	13.246(2)	20.923(3)	9.1011(19)
b/Å	17.865(4)	15.640(2)	17.843(10)	15.526(2)	10.3501(14)	23.816(5)
c/Å	24.564(5)	21.157(3)	24.543(13)	21.175(3)	17.962(3)	19.937(4)
β/°	98.92(3)	105.055(3)	98.901(11)	104.618(4)	111.211(3)	98.592(4)
V/Å^3, Z	6589(2), 8	4244.5(11), 4	6568(6), 8	4214.1(11), 4	3626.2(9), 4	4272.8(16), 4
D_c/g cm^{-3}	1.604	1.471	1.787	1.620	1.618	1.694
μ/mm^{-1}	0.973	0.769	4.094	3.20	0.908	3.467
F(000)	3200	1928	3456	2056	1768	2136
Crystal size/mm	0.20 × 0.16 × 0.14	0.20 × 0.18 × 0.12	0.16 × 0.12 × 0.10	0.20 × 0.16 × 0.14	0.30 × 0.28 × 0.10	0.20 × 0.16 × 0.14
θ Range/°	1.68–27.50	1.64–27.55	1.77–27.60	1.65–27.56	2.09–27.54	2.07–27.60
Limiting indices, hkl	−19 to 13, −15 to 23, −31 to 31	−17 to 12, −20 to 14, −27 to 26	−16 to 19, −21 to 23, −31 to 20	−17 to 11, −19 to 20, −25 to 27	−26 to 27, −13 to 13, −23 to 18	−11 to 11, −30 to 28, −25 to 18
Reflections collected	20989	28358	21041	27228	12074	28667
Independent reflections (R_{int})	7532 (0.0515)	9772 (0.0298)	7411 (0.2278)	9704 (0.0383)	6262 (0.0274)	9832 (0.1499)
Completeness (%) to θ = 27.50°	99.4	99.7	97.2	99.6	99.7	99.4
Absorption correction	SADABS	SADABS	SADABS	SADABS	SADABS	SADABS
Max./min. transmission	0.8758/0.8292	0.9133/0.8613	0.6849/0.5603	0.6631/0.5673	0.9147/0.7724	0.6425/0.5440
Data/restraints/parameters	7532/0/406	9772/0/477	7411/20/400	9704/4/472	6262/23/447	9832/84/468
Goodness-of-fit on F^2	1.028	0.791	1.036	0.695	1.061	0.986
Final R indices [$I > 2\sigma(I)$]	$R1$ = 0.0383, $wR2$ = 0.0790	$R1$ = 0.0335, $wR2$ = 0.0978	$R1$ = 0.0801, $wR2$ = 0.2009	$R1$ = 0.0332, $wR2$ = 0.0913	$R1$ = 0.0353, $wR2$ = 0.0849	$R1$ = 0.0686, $wR2$ = 0.1373
R indices (all data)	$R1$ = 0.0574, $wR2$ = 0.0841	$R1$ = 0.0509, $wR2$ = 0.1159	$R1$ = 0.1240, $wR2$ = 0.2189	$R1$ = 0.0572, $wR2$ = 0.1110	$R1$ = 0.0410, $wR2$ = 0.0878	$R1$ = 0.2343, $wR2$ = 0.1681

Table 2 Selected bond distances (Å) and angles (°) for CpRu(CO)-(μ-dppm)Mo(CO)$_2$Cp (**1**)

Ru(1)–Mo(1)	3.0277(6)	Mo(1)–C(36)	1.949(3)
Ru(1)–P(2)	2.2641(8)	Mo(1)–C(37)	1.934(3)
Mo(1)–P(1)	2.4310(8)	Ru(1)–C(38)	1.845(3)
O(1)–C(36)	1.173(3)	O(2)–C(37)	1.157(4)
O(3)–C(38)	1.158(3)		
P(2)–Ru(1)–Mo(1)	93.18(2)	O(1)–C(36)–Mo(1)	168.9(3)
P(1)–Mo(1)–Ru(1)	84.80(2)	O(2)–C(37)–Mo(1)	174.2(2)
P(2)–C(11)–P(1)	107.30(11)	O(3)–C(38)–Ru(1)	172.8(3)
C(18)–P(1)–Mo(1)	120.74(7)	C(30)–P(2)–Ru(1)	110.56(8)
C(24)–P(2)–Ru(1)	122.60(8)	C(12)–P(1)–Mo(1)	112.48(8)

Table 3 Catalytic hydrogenation of CO_2 with complexes **1**–**4**[a]

Entry	Complex/solvent	Turnover no.[b] (TON)
1	**1**/THF	10
2	**1**/benzene	43
3	**2**/THF	Trace
4	**2**/benzene	Trace
5	**3**/THF	5
6	**3**/benzene	28
7	**4**/THF	Trace
8	**4**/benzene	Trace

[a] Typical reaction conditions: catalyst = 0.009 mmol, solvent: THF or benzene (8 mL), triethylamine (2 mL), H_2 = 30 atm, CO_2 = 30 atm, reaction time = 45 h, temperature = 120 °C. [b] TON = mol of product/mol of complex.

CO_2 hydrogenation to formic acid with 1–4

We monitored the reactions of **1**–**4** with pressurized H_2 (~45 atm) in C_6D_6 at 120 °C for 60 h with high-pressure ^{1}H and ^{31}P{^{1}H} NMR spectroscopy, but we found in each case that the bimetallic complex remained unchanged in the experiment, it was the only NMR observable organometallic species throughout. The sharp singlet signal of dissolved H_2 was observed at δ 4.60 ppm in the ^{1}H NMR spectrum. Although **1**–**4** do not seem to react with H_2 to yield detectable metal hydride species, the bimetallic complexes are able to effect the hydrogenation of CO_2 to formic acid in benzene and THF solutions, albeit in very low yields (Table 3).

We have monitored a **1**-catalyzed CO_2 hydrogenation reaction by high-pressure ^{1}H and ^{31}P{^{1}H} NMR spectroscopy, and have found that **1** was the only observable organometallic species throughout the experiment. Furthermore, we have also learned in separate experiments that the mononuclear systems CpRu(PPh$_3$)(CO)H, CpM(PPh$_3$)(CO)$_2$H, CpRu(dppm)(CO)$^+$, CpRu(dppm)Cl/Ag$^+$ and CpM(CO)$_3^-$ are all inactive in CO_2 hydrogenation reaction. Therefore, it is probably true that the CO_2 hydrogenation reactions with **1**–**4** are heterobimetallic catalytic processes in which fragmentation of the bimetallic systems do not seem to occur.

Formic acid decomposition with 1–4

It is generally true that metal complexes, which are active in catalytic hydrogenation of CO_2 to formic acid, can effect the reverse reaction as well. Table 4 shows the results of formic acid decomposition to CO_2 and H_2 catalyzed by **1**–**4**. Although the catalytic processes are slow, monitoring of the reaction with NMR spectroscopy reveals some interesting results. It was found that after heating a THF-d$_8$ solution containing 2.51 μmol of **1** and 25.1 μmol of formic acid in a sealed 5 mm NMR tube at 80 °C for 2.5 h, the former was partially converted to the hydride complex **5·HCOO**, which was characterized by ^{1}H and ^{31}P{^{1}H} NMR spectroscopy. The ^{31}P{^{1}H} NMR spectrum showed two doublets at δ 39.7 and 48.5 ppm (J(PP) = 56 Hz) for the two phosphorus atoms of dppm. In the ^{1}H NMR spectrum of the hydride complex, the hydride signal at δ −17.16 ppm is a doublet of doublet of doublets (^2J(HP) = 28.2 Hz, ^2J(HP) = 21.0 Hz, J(HH) = 5.4 Hz), it is coupled to the phosphorus atoms and one of the methylene protons of dppm. Coupling of the hydride ligand with one of the methylene protons of dppm is not uncommon.[17] In a double resonance study, irradiation of the dppm methylene signal at δ 4.46 ppm reduced the hydride signal to a doublet of doublets, and conversely irradiating the hydride signal simplified the methylene signal from a multiplet to a pseudo-quartet. The proton signal of the formate cannot be unequivocally identified because it overlaps with the signal of the free formic acid. It is noteworthy that the concentration of **5·HCOO** decreased with the decomposition of formic acid, and it competely reverted to **1** upon the conclusion of the catalytic reaction, as illustrated by ^{1}H and ^{31}P{^{1}H} NMR spectroscopy. Taking the ^{1}H and ^{31}P{^{1}H} NMR data together, it is possible to deduce that the intermediate **5·HCOO** is a dppm-spanned bimetallic complex containing a hydrogen bridge. Reactions of dinuclear metal complexes with acids to form hydride-bridged bimetallic species are well documented.[10b,15,18] For instance, treatment of the dirhodium species [Rh$_2$(CO)$_3$-(dppm)$_2$] with HPF_6 or p-$CH_3C_6H_4SO_3H$ has been shown to lead to the formation of the hydride-bridged bimetallic complex [Rh$_2$(μ-H)(μ-CO)(CO)$_2$(dppm)$_2$]$^+$.[18] The generation of **5·HCOO** was much slower using benzene-d$_6$ in place of THF-d$_8$ as the solvent; **1** was only partially converted to **5·HCOO** after heating the solution at 80 °C for 11 h.

Table 4 Times for complete decomposition of formic acid with **1**–**4**[a]

Entry	Complex/solvent	Reaction time/h
1	**1**/THF-d$_8$	6
2	**1**/C_6D_6	15
3	**2**/THF-d$_8$	16
4	**2**/C_6D_6	24
5	**3**/THF-d$_8$	24
6	**3**/C_6D_6	40
7	**4**/THF-d$_8$	24
8	**4**/C_6D_6	40

[a] Typical experimental conditions: complex 2.51 μmol, solvent 0.4 mL, formic acid 25.1 μmol, temperature 80 °C.

Reactions of 1 and 3 with acids

At this point we digress somewhat to describe the acidification reactions of **1**–**4**. In view of the fact that **1** was not completely converted to **5·HCOO** during the catalytic formic acid decomposition reaction, we reacted **1** with other acids to see if its acidification would go to completion. Stirring a THF solution of **1** with an excess of concentrated hydrochloric acid at room temperature for 30 min led to the formation of the complex **5·Cl**, whose ^{31}P{^{1}H} NMR spectrum is identical to that of **5·HCOO**. The ^{1}H NMR spectrum of **5·Cl** is also identical to that of **5·HCOO** if we ignore the formate and formic acid signals of the latter. Attempts to ascertain the structure of **5·Cl** by X-ray crystallography was frustrated by failure to obtain good single crystals for this purpose. We then reacted **1** with HBF_4·Et$_2$O in THF to obtain the hydride complex **5·BF$_4$**, whose ^{1}H and ^{31}P{^{1}H} NMR spectra are identical to those of **5·Cl**. In view of the identical NMR spectroscopic data of **5·HCOO**, **5·Cl**, and **5·BF$_4$** and the fact that BF_4^- is generally non-coordinating, it is very likely that the three complexes are ionic species with identical cationic portions, but different anions. Unlike **5·Cl**, which resists single crystal growing, **5·BF$_4$** affords single crystals suitable for X-ray diffraction study readily. Fig. 2 shows the molecular structure of the cation [CpRu(CO)-(μ-dppm)(μ-H)Mo(CO)$_2$Cp]$^+$ (**5**$^+$) of **5·BF$_4$**. The structure-refinement information for **5·BF$_4$** can be found in Table 1. Selected bond distances and angles are given in Table 5. The hydride ligand in **5**$^+$ was located and refined to give Mo–H and Ru–H distances of 1.74(6) and 1.87(6) Å, respectively. The

Table 5 Selected bond distances (Å) and angles (°) for [CpRu(CO)(μ-dppm)(μ-H)Mo(CO)$_2$Cp][BF$_4$] (**5·BF$_4$**)

Ru(1)–H	1.87(6)	Mo(1)–H	1.74(6)
Ru(1)–P(1)	2.3053(8)	Mo(1)–P(2)	2.4703(8)
Ru(1)–C(11)	1.880(3)	O(1)–C(11)	1.127(4)
Mo(1)–C(12)	1.982(3)	O(2)–C(12)	1.150(4)
Mo(1)–C(13)	1.953(3)	O(3)–C(13)	1.155(4)
P(1)–C(26)–P(2)	115.07(14)	C(14)–P(1)–Ru(1)	115.58(10)
C(20)–P(1)–Ru(1)	118.90(10)	C(27)–P(2)–Mo(1)	119.63(10)
C(33)–P(2)–Mo(1)	109.87(10)	O(1)–C(11)–Ru(1)	172.0(3)
O(2)–C(12)–Mo(1)	173.3(3)	O(3)–C(13)–Mo(1)	175.0(2)

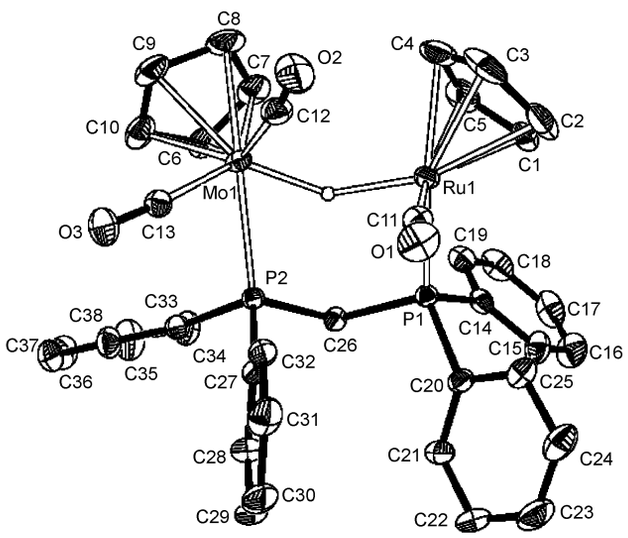

Fig. 2 Molecular structure of [CpRu(CO)(μ-dppm)(μ-H)Mo(CO)$_2$Cp][BF$_4$] (**5·BF$_4$**).

slightly asymmetric position of the bridging hydride in **5**$^+$ is manifested by the unequal H–P coupling constants exhibited by the hydride signal in the ^{1}H NMR spectrum. It was reported that the hydride signals which showed unequal H–P coupling constants in the complexes [Ru(CO)$_2$(μ-H)(μ-dppm)$_2$Mo(CF$_3$COO)(CO)$_3$][10b] and [Ir$_2$(μ-H)(μ-Pz)$_2$H$_3$(NCCH$_3$)(P^{i}Pr$_3$)$_2$],[19] are consistent with the bridging hydride ligands being not equidistant from the metal centers. All carbonyl groups in **5**$^+$ are terminal, in consonance with the IR spectrum of **5·BF$_4$** or **5·Cl**, which shows no carbonyl stretch below 1880 cm^{-1}. The metal centers in **5**$^+$ are separated by a distance of 3.277(6) Å, although it is longer than that of the parent complex **1**, it cannot exclude the existence of metal–metal bond in the complex. The presence of a three-center–two-electron bond is highly probable. In congruence with the large metal–metal separation, the P–C–P angle of the dppm ligand in **5**$^+$ is much larger than that in the parent complex **1** [115.07(14) *vs.* 107.30(11)°].

Reaction of **3** with an excess of concentrated hydrochloric acid in THF at room temperature yielded the protonated complex **6·Cl**, which is analogous to **5·Cl**. The structure of **6**$^+$ is very similar to that of **5**$^+$ (For the characterization and X-ray structure determination of **6·Cl**, see ESI †).

It is noteworthy that the chloride anions in **5·Cl** and **6·Cl** are non-coordinating, probably for steric reasons. Although the protonation reactions of **1** and **3** to give **5·Cl** and **6·Cl**, respectively, were carried out in the presence of an excess of concentrated hydrochloric acid, further protonation of **5·Cl** and **6·Cl** did not occur. Similarly, reaction of **5** and **6** with an excess of HBF$_4$·Et$_2$O or triflic acid only gave the mono-protonated products **5·BF$_4$** (or **5·OTf**) and **6·BF$_4$** (or **6·OTf**), respectively, again no further protonation was observed. It has been reported that CpW(CO)$_2$(PR$_3$)H (R = Me, Cy, Ph) can be protonated by strong acids such as HOTf and [H(Et$_2$O)$_2$]$^+$BAr′$_4^-$ (Ar′ = 3,5-bis(trifluoromethyl)phenyl) to give the dihydrides [CpW(CO)$_2$(PR$_3$)H$_2$]$^+$OTf$^-$ and [CpW(CO)$_2$(PR$_3$)H$_2$]$^+$BAr′$_4^-$, respectively.[20] The molybdenum dihydride [CpMo(CO)$_2$(PR$_3$)H$_2$]$^+$ has been implicated as an intermediate in catalytic ionic hydrogenation, but has not been directly observed.[21] It has also been reported that reaction of diphosphazane-bridged derivatives of nonacarbonyldiruthenium, [Ru$_2$(μ-CO)(CO)$_4${μ-(RO)$_2$PN(Et)-P(OR)$_2$}$_2$] (R = Me or Pr^i) with HCl and HBr first gives the hydride species [Ru$_2$H(CO)$_5${μ-(RO)$_2$PN(Et)P(OR)$_2$}$_2$]$^+$, which further reacts with the acid to produce the halogeno-bridged complexes [Ru$_2$(μ-X)(CO)$_5${μ-(RO)$_2$PN(Et)P(OR)$_2$}$_2$]$^+$ (X = Cl, Br). In these reactions, the acids, in a formal sense, exhibit a type of *umpolung* behavior.[22]

Reactions of 5·OTf with Ph$_3$C$^+$OTf$^-$ and Me$_3$Si$^+$OTf$^-$

In their study of catalytic ionic hydrogenation of ketones with molybdenum and tungsten catalysts, Bullock and Voges generated the catalyst precursors [CpM(PR$_3$)(CO)$_2$(O=CEt$_2$)]$^+$ (M = Mo, W) by abstracting the hydrogen of the M–H bond of CpM(PR$_3$)(CO)$_2$H as a hydride with Ph$_3$C$^+$ in the presence of 3-pentanone.[21] The bridging hydrogen atom in **5·OTf**, however, could not be removed by the action of Ph$_3$C$^+$OTf$^-$. Similarly, **5·OTf** failed to react with Me$_3$Si$^+$OTf$^-$.

Reactions of 5·BF$_4$ with bases

After our attempts to remove the bridging hydrogen atom of **5·BF$_4$** as a hydride ligand failed, we tested the reactivity of the complex towards the weak base Et$_3$N. It was found that **5·BF$_4$** remained intact after refluxing a THF solution of the complex in the presence of an excess of Et$_3$N for 45 h. However, **1** was regenerated when **5·BF$_4$** was allowed to react with the strong base sodium methoxide (eqn. (2)).

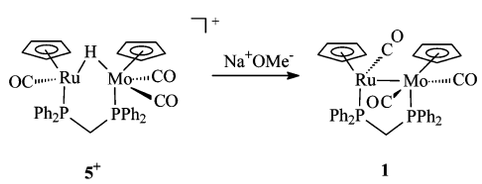

Reactions of 5·BF$_4$ and 5·Cl with Et$_3$SiH

We anticipate that reaction of **5**$^+$ with silane would provide a silyl complex, which may demonstrate some interesting characteristics. Complex **5·BF$_4$** was reacted with triethylsilane in THF; however, the complex remained unchanged after refluxing the solution for 24 h. On the other hand, **5·Cl** behaved quite differently, its reaction with Et$_3$SiH yielded **1** and chlorotriethylsilane; the latter was detected by ^{29}Si{^{1}H} NMR spectroscopy.

Reaction of 5·Cl with Na$^+$BPh$_4^-$

Since it was difficult to obtain single crystals of **5·Cl** for X-ray diffraction study, we had tried to change the chloride anion to tetraphenylborate by reacting **5·Cl** with a stoichiometric amount of Na$^+$BPh$_4^-$. However, instead of yielding the expected complex, the reaction regenerated **1** quantitatively, along with the formation of BPh$_3$ and benzene, which were detected by ^{11}B{^{1}H} and ^{1}H NMR spectroscopy, respectively (eqn. (3)). The reaction depicted in eqn. (3) results from

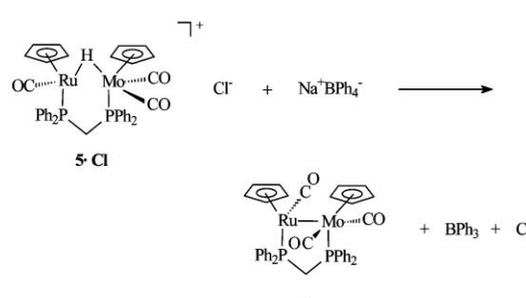

acidification of BPh_4^-, suggestive of the acidic nature of the bridging hydrogen of **5·Cl**. Proton-induced cleavage of an aryl group from tetraarylborates is well-documented.[23]

Possible mechanism for CO_2 hydrogenation and formic acid decomposition catalyzed by 1–4

In a metal complex-catalyzed CO_2 hydrogenation reaction, activation of the H_2 molecule by the metal center is an important step. Although no metal hydride species were detectable by ^1H and $^{31}P\{^1H\}$ NMR spectroscopy in the **1**–**4** catalyzed CO_2 hydrogenation reactions, we propose that a metal hydride intermediate is generated as a transient species during the catalysis (species **B** in Scheme 1). It is present in very low concentration or is very short-lived, so that it evades observation by NMR spectroscopy. Since the hydride on ruthenium is more hydridic[24] and the one on M is more acidic,[26] the Ru–H ··· H–M dihydrogen bond is likely to be present in **B**. Reaction of **B** with CO_2 yields the intermediate **C**, and it does not accumulate to such a concentration that it is detectable by NMR spectroscopy in the hydrogenation reaction. The low catalytic activities of **1**–**4** in CO_2 hydrogenation can probably be attributed to the non-facile generation of the hydride intermediate **B**.

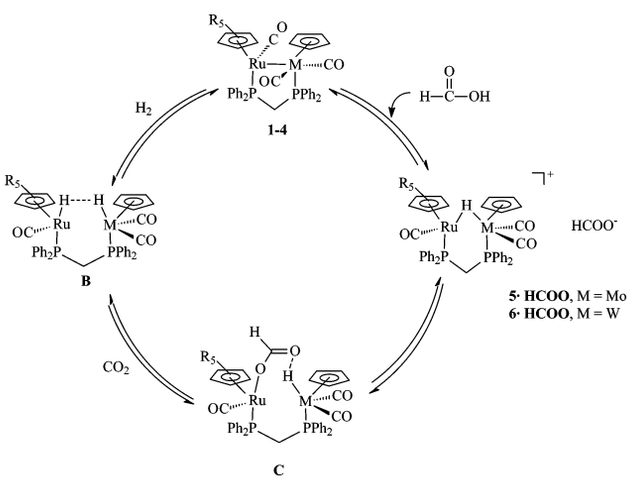

Scheme 1 Proposed mechanism of CO_2 hydrogenation and decomposition of formic acid catalysed by **1**–**4**.

The catalysis of formic acid decomposition is proposed to proceed by the same catalytic cycle, but in a reversed manner. That the intermediate **5** or **6** can be detected by NMR spectroscopy in the early stage of the decomposition reaction is probably due to the presence of relatively high concentration of HCOOH, therefore shifting the equilibrium towards **5** or **6**.

Further support of the proposed mechanism for formic acid decomposition in Scheme 1 could be obtained from the reactions of **5·OTf** and **6·OTf** with sodium formate. After heating a THF-d_8 solution of **5·OTf** (or **6·OTf**) with one equiv. of sodium formate in a sealed NMR tube at 80 °C for 6 h, $^{31}P\{^1H\}$ NMR spectroscopy showed that the metal–metal bonded complex **1** (or **3**) was regenerated. ^1H NMR spectroscopy showed the disappearance of the signal of the formate ion and the appearance of the signal of free H_2 (δ 4.60 ppm). One of the reasons for the sluggishness of the formic acid decomposition by **1**–**4** is probably the difficulty encountered by the formate anion in opening up the hydrogen bridge, direct hydride delivery from the formate to the M–H might also be non-facile.

Conclusion

The main thrust of this work is to synthesize Ru–Mo and Ru–W bimetallic complexes (**1**–**4**) and study the activation of H_2 with these complexes. We hope, by virtue of the greater hydridicity of the Ru–H and the higher acidity of the M–H (M = Mo or W), we would be able to generate interesting bimetallic systems containing the dihydrogen-bonded moiety Ru–H ··· H–M. Unfortunately, we have not been able to observe these dihydrogen-bonded dihydride species in the *in-situ* high-pressure NMR studies of the reactions of **1**–**4** with H_2. However, **1**–**4** show activity (albeit very low) in the catalysis of CO_2 hydrogenation to formic acid and the reverse reaction, *i.e.*, the decomposition of formic acid to H_2 and CO_2. A reaction mechanism, involving the transient intermediacy of the dihydrogen-bonded dihydride species, is proposed to account for the catalytic reactions. We attribute the low activity of **1**–**4** in CO_2 hydrogenation to their non-facile reactions with H_2 to generate the active dihydride species; on the other hand, the sluggishness of the catalytic formic acid decomposition by these bimetallic complexes is probably due to the formation of a stable intermediate, which contains a strong Ru–H–M bridge.

Experimental

All reactions were carried out under a dry N_2 atmosphere using standard Schlenk techniques. All solvents were distilled and degassed prior to use. Dichloromethane was distilled from calcium hydride. Tetrahydrofuran, diethyl ether, toluene and hexane were distilled from sodium–benzophenone ketyl. Methanol and ethanol were distilled from magnesium and iodine. CpRu(dppm)Cl,[28] $CpMo(CO)_3^-Na^+$,[29] and $CpW(CO)_3^-Na^+$ [29] were synthesized according to published procedures. Formic acid and sodium formate were purchased from BDH and used as received. Trifluoromethanesulfonic acid and $HBF_4.Et_2O$ were purchased from Aldrich.

Infrared spectra were obtained from a Bruker Vector 22 FT-IR spectrophotometer. ^1H NMR spectra were obtained from a Bruker DPX 400 spectrometer. Chemical shifts (δ, ppm) were measured relative to the proton residue of the deuterated solvent (THF-d_8 δ 1.85 ppm, CD_3COCD_3 δ 2.20 ppm, C_6D_6 δ 7.40 ppm.) $^{31}P\{^1H\}$ NMR spectra were taken on a Bruker DPX-400 spectrometer at 161.98 MHz. $^{31}P\{^1H\}$ NMR chemical shifts were externally referenced to 85% H_3PO_4 in D_2O (δ 0.00 ppm). $^{29}Si\{^1H\}$ NMR spectra were taken on a Bruker DPX-400 spectrometer at 79.5 MHz. $^{11}B\{^1H\}$ NMR spectra were taken on a Bruker DPX-400 spectrometer at 128.3 MHz. High-pressure NMR studies were carried out in a sapphire HP NMR tube; the 10 mm sapphire NMR tube was purchased from Saphikon, Milford, NH, and the titanium high-pressure valve was constructed at the ISSECC-CNR, Firenze, Italy. Electrospray Ionization Mass Spectrometry was carried out with a Finnigan MAT 95S mass spectrometer by first dissolving the sample in CH_2Cl_2–MeOH. Elemental analyses were performed by M–H–W Laboratories, Phoenix, AZ, USA.

CpRu(CO)(μ-dppm)Mo(CO)$_2$Cp (1)

Degassed THF (8 mL) was added to a solid mixture of $CpMo(CO)_3Na$ (0.10 g, 0.38 mmol) and CpRu(dppm)Cl (0.22 g, 0.38 mmol), the reaction mixture was heated at 120 °C for 48 h, during which, the color of the solution changed from orange to dark red. The resulting solution was then filtered to remove the salt formed. Upon removal of the solvent of the filtrate under vacuum, 5 mL of hexane was added to the residual paste with vigorous stirring to produce a red solid, which was collected by filtration. The solid was washed with methanol (2 × 2 mL) and diethyl ether (2 × 2 mL) and then dried *in vacuo*. Yield: 0.22 g (73%). Anal. Calc. for $RuMoC_{38}H_{32}O_3P_2$: C 57.37, H 4.05. Found: C 56.98, H 4.02%. IR (KBr, cm^{-1}): ν(C≡O) 1791 (m), 1873 (s) and 1894 (sh). ^1H NMR (400.13 MHz, C_6D_6, 25 °C): δ 3.85 (m, 1H, PC*H*HP), 4.50 (m, 1H, PCH*H*P), 5.06 (s, 5H, CpRu), 5.08 (s, 5H, CpMo), 7.02–7.76 (m, 20H of dppm). $^{31}P\{^1H\}$ NMR (161.99 MHz, C_6D_6, 25 °C): δ 49.9 [d, ^2J(PP) =

75.6 Hz], 53.7 [d, ^2J(PP) = 75.6 Hz]. ESI-MS (CH_2Cl_2–MeOH as solvent) *m*/*z*: 795 $[M]^+$.

Cp*Ru(CO)(μ-dppm)Mo(CO)$_2$Cp (2)

The procedure for **1** was followed exactly, except that Cp*Ru(dppm)Cl was used in place of CpRu(dppm)Cl. Yield: 0.21 g (70%). Anal. Calc. for $RuMoC_{43}H_{37}O_3P_2$: C 60.00, H 4.33. Found: C 59.74, H 4.52%. IR (KBr, cm^{-1}): ν(C≡O) 1777 (m), 1854 (s) and 1874 (sh). ^{1}H NMR (400.13 MHz, C_6D_6, 25 °C): δ 1.50 (s, 15H, methyls of Cp*) δ 2.87 (m, 1H, PC*H*HP), 3.67 (m, 1H, PCH*H*P), 5.06 (s, 5H, CpMo), 7.00–7.50 (m, 20H of dppm). ^{31}P{^{1}H} NMR (161.99 MHz, C_6D_6, 25 °C): δ 46.9 [d, ^2J(PP) = 76.1 Hz], 58.9 [d, ^2J(PP) = 76.1 Hz]. ESI-MS (CH_2Cl_2–MeOH as solvent) *m*/*z*: 865 $[M]^+$.

CpRu(CO)(μ-dppm)W(CO)$_2$Cp (3)

This complex was prepared by using the same procedure as for the preparation of **1**, except that $CpW(CO)_3Na$ was used instead of $CpMo(CO)_3Na$. Yield: 0.21 g (78%). Anal. Calc. for $RuWC_{38}H_{32}O_3P_2$: C 51.66, H 3.65. Found: C 51.30, H 3.58%. IR (KBr, cm^{-1}): ν(C≡O) 1792 (s), 1872 (s) and 1892 (sh). ^{1}H NMR (400.13 MHz, C_6D_6, 25 °C): δ 4.21 (m, 1H, PC*H*HP), 4.55 (m, 1H, PCH*H*P), 5.03 (s, 5H, CpRu), 5.04 (s, 5H, CpMo), 6.90–7.79 (m, 20H of dppm). ^{31}P{^{1}H} NMR (161.99 MHz, C_6D_6, 25 °C): δ 21.1 [d, ^2J(PP) = 74.3 Hz], 56.1 [d, ^2J(PP) = 74.3 Hz]. ESI-MS (CH_2Cl_2–MeOH as solvent) *m*/*z*: 881 $[M]^+$.

Cp*Ru(CO)(μ-dppm)W(CO)$_2$Cp (4)

This complex was prepared by using the same procedure as for the preparation of **3** except that Cp*Ru(dppm)Cl was used in place of CpRu(dppm)Cl. Yield: 0.23 g (76%). Anal. Calc. for $RuWC_{43}H_{37}O_3P_2$: C 54.44, H 3.93. Found: C 54.32, H 4.02%. IR (KBr, cm^{-1}): ν(C≡O) 1784 (med), 1854 (s) and 1873 (sh). ^{1}H NMR (400.13 MHz, C_6D_6, 25 °C): δ 1.55 (s, 15H, methyls of Cp*) δ 2.88 (m, 1H, PC*H*HP), 3.66 (m, 1H, PCH*H*P), 4.84 (s, 5H, CpMo), 6.76–7.29 (m, 20H of dppm). ^{31}P{^{1}H} NMR (161.99 MHz, C_6D_6, 25 °C): δ 21.3 [d, ^2J(PP) = 72.9 Hz], 48.2[d, ^2J(PP) = 72.9 Hz]. ESI-MS (CH_2Cl_2–MeOH as solvent) *m*/*z*: 951 $[M]^+$.

Hydrogenation of CO_2 by 1–4

The reactions were carried out in a 250 mL stainless steel autoclave. In a typical run, 0.009 mmol of the complex was dissolved in 8 mL of THF or benzene and 2 mL of triethylamine was added. The solution was heated under 60 atm of CO_2/H_2 (30 atm/30 atm) at 120 °C for 45 h. The reactor was cooled rapidly and carefully vented. Formic acid formed was analyzed by ^{1}H NMR spectroscopy, with DMF (0.5 μL) as internal standard.

Decomposition of formic acid by 1–4

The reactions were performed in a 5 mm NMR tube and were monitored by ^{1}H and ^{31}P{^{1}H} NMR spectroscopy. In a typical run, 2.51 μmol of the complex was dissolved in 0.4 mL of C_6D_6 or THF-d_8 in a 5 mm NMR tube. 10 equiv of formic acid (0.964 μL, 0.0251 mmol) was then added and the mixture was heated at 80 °C. The progress of the decomposition reaction was monitored by ^{1}H NMR spectroscopy in 2 h intervals.

Preparation of [CpRu(CO)(μ-dppm)(μ-H)Mo(CO)$_2$Cp]$^+$[Cl]$^-$ (5·Cl)

Complex **1** (0.020 g, 0.025 mmol) was dissolved in 10 mL of THF. An excess of concentrated HCl (37%, aq) (0.5 mL) was added to the solution and the mixture was stirred for 30 min. Solvent was removed under vacuum. Hexane (5 mL) was added to the residue, with stirring, to produce an orange solid. This was collected and washed with water (2 × 1 mL) and diethyl ether (2 × 2 mL), and dried under vacuum. Yield: 0.016 g (80%). Anal. Calc. for $RuMoC_{38}H_{33}ClO_3P_2$: C 54.85, H 4.00. Found: 54.79, H 3.94%. IR (KBr, cm^{-1}): ν(C≡O). 1880 (s), 1949 (sh) and 1972 (s). ^{1}H NMR (400.13 MHz, THF-d_8, 25 °C): δ −17.16 [ddd, ^2J(HP) = 28.0 Hz, ^2J(HP) = 20.8 Hz, J(HH) = 5.6 Hz, 1H, Mo–H–Ru], 3.90 (m, 1H, PC*H*HP), 4.42 (m, 1H, PCH*H*P), 5.20 (s, 5H, CpRu), 5.56 (s, 5H, CpMo), 7.10–7.77 (m, 20H of dppm). ^{31}P{^{1}H} NMR (161.99 MHz, THF-d_8, 25 °C): δ 39.7 [dd, ^2J(PP) = 56.4 Hz, J(HH) = 13.1 Hz], 48.4 [dd, ^2J(PP) = 56.4 Hz, J(HH) = 13.1 Hz]. ESI-MS (CH_2Cl_2–MeOH as solvent) *m*/*z*: 832 $[M]^+$.

Synthesis of [CpRu(CO)(μ-dppm)(μ-H)Mo(CO)$_2$Cp]$^+$[BF$_4$]$^-$ (5·BF$_4$)

Complex **1** (0.020 g, 0.025 mmol) was dissolved in 10 mL of THF in a Schlenk flask. $HBF_4{\cdot}Et_2O$ (54%, 6.9 μL, 0.050 mmol) was added and the resulting solution was heated at 80 °C for 2 h. Solvent was removed under vacuum. Hexane (5 mL) was added to the residue, with stirring, to produce an orange solid. This was collected and washed with water (2 × 1 mL) and diethyl ether (2 × 2 mL), and dried under vacuum. Yield: 0.017 g (77%). The product was identified by ^{1}H and ^{31}P{^{1}H} NMR spectroscopy. ^{1}H NMR (400.13 MHz, THF-d_8, 25 °C): δ −17.16 [ddd, ^2J(HP) = 28.2 Hz, ^2J(HP) = 21.0 Hz, J(HH) = 5.6 Hz, 1H, Mo–H–Ru], 3.98 (m, 1H, PC*H*HP), 4.46 (m, 1H, PCH*H*P), 5.16 (s, 5H, CpRu), 5.61 (s, 5H, CpMo), 7.05–7.72 (m, 20H of dppm). ^{31}P{^{1}H} NMR (161.99 MHz, THF-d_8, 25 °C): δ 39.7 [d, ^2J(PP) = 56.3 Hz], 48.5 [d, ^2J(PP) = 56.3 Hz].

Synthesis of [CpRu(CO)(μ-dppm)(μ-H)Mo(CO)$_2$Cp]$^+$[OTf]$^-$ (5·OTf)

The procedure for preparation of **5·OTf** is similar to that of **5·BF$_4$**, except that trifluoromethanesulfonic acid (4.40 μL, 0.050 mmol) was used instead of $HBF_4{\cdot}Et_2O$. Yield: 0.019 g (80%) ^{1}H NMR (400.13 MHz, THF-d_8, 25 °C): δ −17.17 [ddd, ^2J(HP) = 28.8 Hz, ^2J(HP) = 21.0 Hz, J(HH) = 5.6 Hz, 1H, Mo–H–Ru], 3.98 (m, 1H, PC*H*HP), 4.46 (m, 1H, PCH*H*P), 5.20 (s, 5H, CpRu), 5.65 (s, 5H, CpMo), 7.09–7.61 (m, 20H of dppm). ^{31}P{^{1}H} NMR (161.99 MHz, THF-d_8, 25 °C): δ 39.7 [d, ^2J(PP) = 56.3 Hz], 48.5 [d, ^2J(PP) = 56.3 Hz].

Synthesis of [CpRu(CO)(μ-dppm)(μ-H)W(CO)$_2$Cp]$^+$[Cl]$^-$ (6·Cl)

Complex **3** (0.020 g, 0.023 mmol) was dissolved in 10 mL of THF, and an excess of concentrated HCl (37%, aq.) (0.5 mL) was added. The solution was stirred for 30 min, and the solvent was removed under vacuum. Hexane (5 mL) was added to the residue, with stirring, to produce an orange solid. The solid was collected and washed with water (2 × 1 mL) and diethyl ether (2 × 2 mL), and then dried under vacuum. Yield: 0.016 g (78%). Anal. Calc. for $RuWC_{38}H_{33}ClO_3P_2$: C 49.61, H 3.62. Found: C 49.64, H 3.81%. IR (KBr, cm^{-1}): ν(C≡O). 1867 (m), 1947 (sh) and 1972 (s). ^{1}H NMR (400.13 MHz, THF-d_8, 25 °C): δ −17.72 [ddd, ^2J(HP) = 27.6 Hz, ^2J(HP) = 19.2 Hz, J(HH) = 5.2 Hz, 1H, W–H–Ru; in the phosphorus-decoupled ^{1}H NMR spectrum, the W satellites of the bridging hydride signal were observed, J(HW) = 47 Hz], 3.91 (m, 1H, PC*H*HP), 4.89 (m, 1H, PCH*H*P), 5.20 (s, 5H, CpRu), 5.66 (s, 5H, CpW), 7.10–7.61 (m, 20H of dppm). ^{31}P{^{1}H} NMR (161.99 MHz, THF-d_8, 25 °C): δ 14.3 [dd, ^2J(PP) = 53.5 Hz, J(HH) = 10.7 Hz], 40.5 [dd, ^2J(PP) = 53.5 Hz, J(HH) = 10.7 Hz]. ESI-MS (CH_2Cl_2–MeOH as solvent) *m*/*z*: 884 $[M - Cl]^+$.

Synthesis of [CpRu(CO)(μ-dppm)(μ-H)W(CO)$_2$Cp]$^+$[BF$_4$]$^-$ (6·BF$_4$)

Complex **3** (0.020 g, 0.023 mmol) was dissolved in 10 mL of THF. $HBF_4{\cdot}Et_2O$ (54%, 6.3 μL, 0.046 mmol) was added and the solution was heated at 80 °C for 2 h. Solvent was removed under vacuum. Hexane (5 mL) was added to the residue, with stirring,

to produce an orange solid. This was collected and washed with water (2 × 1 mL) and diethyl ether (2 × 2 mL), and dried under vacuum. Yield: 0.019 g (78%). The product was then identified by ^{1}H and ^{31}P{^{1}H} NMR spectroscopy. ^{1}H NMR (400.13 MHz, THF-d_8, 25 °C): δ −17.72 [ddd, ^{2}J(HP) = 27.6 Hz, ^{2}J(HP) = 19.2 Hz, J(HH) = 5.2 Hz, 1H, W–H–Ru; in the phosphorus-decoupled ^{1}H NMR spectrum, the W satellites of the bridging hydride signal were observed, J(HW) = 47 Hz], 3.91 (m, 1H, PC*H*HP), 4.89 (m, 1H, PCH*H*P), 5.20 (s, 5H, CpRu), 5.66 (s, 5H, CpW), 7.10–7.61 (m, 20H of dppm). ^{31}P{^{1}H} NMR (161.99 MHz, THF-d_8, 25 °C): δ 14.3 [dd, ^{2}J(PP) = 53.5 Hz, J(HH) = 10.7 Hz], 40.5 [dd, ^{2}J(PP) = 53.5 Hz, J(HH) = 10.7 Hz].

Synthesis of [CpRu(CO)(μ-dppm)(μ-H)W(CO)$_2$Cp]$^+$[OTf]$^-$ (6·OTf)

The procedure for preparation of **6·OTf** is similar to that of **6·BF$_4$**, except that trifluoromethanesulfonic acid (4.10 μL, 0.046 mmol) was used instead of HBF$_4$·Et$_2$O. Yield: 0.020 g (77%). ^{1}H NMR (400.13 MHz, THF-d_8, 25 °C): δ −17.72 [ddd, ^{2}J(HP) = 27.6 Hz, ^{2}J(HP) = 19.2 Hz, J(HH) = 5.2 Hz, 1H, W–H–Ru; in the phosphorus-decoupled ^{1}H NMR spectrum, the W satellites of the bridging hydride signal were observed, J(HW) = 47 Hz], 3.91 (m, 1H, PC*H*HP), 4.89 (m, 1H, PCH*H*P), 5.20 (s, 5H, CpRu), 5.66 (s, 5H, CpW), 7.10–7.61 (m, 20H of dppm). ^{31}P{^{1}H} NMR (161.99 MHz, THF-d_8, 25 °C): δ 14.3 [dd, ^{2}J(PP) = 53.5 Hz, J(HH) = 10.7 Hz], 40.5 [dd, ^{2}J(PP) = 53.5 Hz, J(HH) = 10.7 Hz].

Reaction of 5·Cl with sodium methoxide

Sodium methoxide was prepared by reacting sodium metal (0.5 g) with methanol (10 mL). After all the sodium metal was reacted, the sodium methoxide solution was transferred to another Schlenk flask loaded with complex **5·Cl** (0.18 g, 0.22 mmol). The mixture was refluxed for 16 h after which the solvent was removed under vacuum. Hexane (10 mL) was added to the residue with stirring to obtain a red solid, which was found to be **1** by ^{1}H and ^{31}P{^{1}H} NMR spectroscopy.

Reaction of 5·Cl with Et$_3$SiH

A sample of **5·Cl** (0.0013 g, 1.56 μmol) was dissolved in THF-d_8 (0.5 mL) in a 5 mm NMR tube and triethylsilane (0.25 μL, 1.56 μmol) was added. The mixture was then refluxed for 24 h. The resulting mixture was analyzed at room-temperature by ^{1}H, ^{31}P{^{1}H} and ^{29}Si{^{1}H} NMR spectroscopy. ^{1}H NMR (400.13 MHz, THF-d_8, 25 °C): δ 0.63 (q, J(HH) = 7.8 Hz, 2H, SiCH$_2$), 1.07 (t, J(HH) = 7.8 Hz, 3H, SiCH$_2$C*H*$_3$), 3.85 (m, 1H, PC*H*HP), 4.50 (m, 1H, PCH*H*P), 5.06 (s, 5H, CpRu), 5.08 (s, 5H, CpMo), 7.02–7.76 (m, 20H of dppm). ^{31}P{^{1}H} NMR (161.99 MHz, THF-d_8, 25 °C): δ 49.9 [d, ^{2}J(PP) = 75.6 Hz], 53.7 [d, ^{2}J(PP) = 75.6 Hz]. ^{29}Si{^{1}H} NMR (79.5 MHz, THF-d_8, 25 °C): δ 20.8.

Reaction of 5·Cl with sodium tetraphenylborate

Complex **5·Cl** (0.0032 g, 3.85 μmol) and sodium tetraphenylborate (0.0013 g, 3.85 μmol) were dissolved in THF-d_8 (0.5 mL) in a 5 mm NMR tube. The solution was heated at 95 °C for 4 h. The resulting mixture was analyzed by room-temperature ^{1}H, ^{11}B{^{1}H} and ^{31}P{^{1}H} NMR spectroscopy. The ^{1}H and ^{31}P{^{1}H} NMR spectroscopic results showed that complex **1** was regenerated. The formation of triphenylborane was confirmed by ^{11}B{^{1}H} NMR. ^{11}B{^{1}H} NMR (128.4 MHz, THF-d_8, 25 °C): δ 68.8.

Reaction of [CpRu(CO)(μ-dppm)(μ-H)Mo(CO)$_2$Cp]$^+$OTf$^-$ (5·OTf) with sodium formate

The complex [CpRu(CO)(μ-dppm)(μ-H)Mo(CO)$_2$Cp]$^+$OTf$^-$ (**5**·OTf) (0.0020 g, 2.1 μmol) and a five-fold excess of sodium formate (0.9 mg, 10.5 μmol) were dissolved in THF-d_8 (0.5 mL) in a NMR tube. The mixture was then allowed to heat at 80 °C for 6 h. The reaction products were identified by ^{1}H and ^{31}P{^{1}H} NMR spectroscopy.

Reaction of [CpRu(CO)(μ-dppm)(μ-H)W(CO)$_2$Cp]$^+$OTf$^-$ (6·OTf) with sodium formate

The procedure of this reaction is the same as that of [CpRu(CO)(μ-dppm)(μ-H)Mo(CO)$_2$Cp]$^+$OTf$^-$ (**5·OTf**), except that [CpRu(CO)(μ-dppm)(μ-H)W(CO)$_2$Cp]$^+$OTf$^-$ (**6·OTf**) was used in place of [CpRu(CO)(μ-dppm)(μ-H)Mo(CO)$_2$Cp]$^+$OTf$^-$ (**5·OTf**).

Crystallographic analysis for CpRu(CO)(μ-dppm)Mo(CO)$_2$Cp (1), Cp*Ru(CO)(μ-dppm)Mo(CO)$_2$Cp (2), CpRu(CO)(μ-dppm)-W(CO)$_2$Cp(3),Cp*Ru(CO)(μ-dppm)W(CO)$_2$Cp(4),[CpRu(CO)-(μ-dppm)(μ-H)Mo(CO)$_2$Cp]$^+$[BF$_4$]$^-$ (5·BF$_4$) and [CpRu(CO)-(μ-dppm)(μ-H)W(CO)$_2$Cp]$^+$[Cl]$^-$ (6·Cl)

Crystals suitable for an X-ray diffraction study for **1**,**3**, **5·BF$_4$**, and **6·Cl** were obtained by layering of hexane on CH_2Cl_2 solutions of these complexes, while crystals of **2** and **4** were obtained by layering of diethyl ether on their CH_2Cl_2 solutions. A suitable crystal of each of the complexes was mounted on a Bruker CCD area detector diffractometer using Mo-Kα radiation (λ = 0.71073 Å) from a generator operating at 50 kV and 30 mA. The intensity data of **1**–**4**, **5·BF$_4$** and **6·Cl** were collected in the 2θ range 3–55°, with oscillation frames of ϕ and ω in the range 0–180°. 1321 Frames were taken in four shells. An empirical absorption correction of the SADABS (G. M. Sheldrick, 1996) program based on Fourier coefficient fitting was applied. The crystal structures were determined by the direct method, which yielded the positions of part of the non-hydrogen atoms, and subsequent difference Fourier syntheses were employed to locate all of the remaining non-hydrogen atoms which did not show up in the initial structure. Hydrogen atoms were located based on difference Fourier syntheses connecting geometrical analysis. All non-hydrogen atoms were refined anisotropically with weight function $w = 1/[\sigma^2(F_o^2) + 0.1000p]^2 + 0.0000p]$, where $p = (F_o^2 + 2F_c^2)/3$ were refined. Hydrogen atoms were refined with fixed individual displacement parameters. All experiment and computation were performed on a Bruker CCD Area Detector Diffractometer and PC computer with program of Bruker Smart and Bruker SHELXTL packages.

CCDC reference numbers 211626–211631.

See http://www.rsc.org/suppdata/dt/b3/b306835h/ for crystallographic data in CIF or other electronic format.

Acknowledgements

We thank the Hong Kong Polytechnic University for financial support.

References and notes

1 (*a*) M. Ito, M. Hirakawa, K. Murata and T. Ikariya, *Organometallics*, 2001, **20**, 379; (*b*) K. Abdur-Rashid, A. J. Lough and R. H. Morris, *Organometallics*, 2000, **19**, 2655; (*c*) K. Abdur-Rashid, D. G. Gusev, A. J. Lough and R. H. Morris, *Organometallics*, 2000, **19**, 834; (*d*) S. Gründemann, S. Ulrich, H.-H. Limbach, N. S. Golubev, G. S. Denisov, L. M. Epstein, S. Sabo-Etienne and B. Chaudret, *Inorg. Chem.*, 1999, **38**, 2550; (*e*) A. Caballero, F. A. Jalón and B. R. Manzano, *Chem. Commun.*, 1998, 1879; (*f*) M. G. Basallote, J. Durán, J. Fernández-Trujillo, M. A. Máñez and J. R. de la Torre, *J. Chem. Soc., Dalton Trans.*, 1998, 745; (*g*) J. A. Ayllón, C. Gervaux, S. Sabo-Etienne and B. Chaudret, *Organometallics*, 1997, **16**, 2000; (*h*) M. Schlaf and R. H. Morris, *J. Chem. Soc., Chem. Commun.*, 1995, 625; (*i*) J. C. Lee Jr., E. Peris, A. L. Rheingold and R. H. Crabtree, *J. Am. Chem. Soc.*, 1994, **116**, 11014.

2 (*a*) R. Custelcean and J. E. Jackson, *Chem. Rev.*, 2001, **101**, 1963; (*b*) K. Abdur-Rashid, M. Faatz, A. J. Lough and R. H. Morris,

J. Am. Chem. Soc., 2001, **123**, 7473; (*c*) M. M. Abad, I. Atheaux, A. Maisonnat and B. Chaudret, *Chem. Commun.*, 1999, 381; (*d*) S. Aime, M. Férriz, R. Gobetto and E. Valls, *Organometallics*, 1999, **18**, 2030; (*e*) Y. Guari, J. A. Ayllón, S. Sabo-Etienne and B. Chaudret, *Inorg. Chem.*, 1998, **37**, 640; (*f*) S. Aime, R. Gobetto and E. Valls, *Organometallics*, 1997, **16**, 5140; (*g*) W. Yao and R. H. Crabtree, *Inorg. Chem.*, 1996, **35**, 3007; (*h*) J. C. Lee, Jr., A. L. Rheingold, B. Muller, P. S. Pregosin and R. H. Crabtree, *J. Chem. Soc., Chem. Commun.*, 1994, 1021.

3 H. S. Chu, C. P. Lau, K. Y. Wong and W. T. Wong, *Organometallics*, 1998, **17**, 2768.

4 (*a*) R. D. Adams and F. A. Cotton, *Catalysis by Di- and Polynuclear Metal Complexes*, Wiley-VCH, New York, 1998; (*b*) P. Braunstein, J. Rose, in *Comprehensive Organometallic Chemistry*, ed. E. W. Abel, F. G. A. Stone and G. Wilkinson, Pergamon, Oxford, 2nd edn., 1995, vol. 10, ch. 7.

5 See, for example: (*a*) F. Torres, E. Sola, A. Elduque, A. R. Martínez, F. J. Lohoz and L. A. Oro, *Chem. Eur. J.*, 2000, **6**, 2120; (*b*) Y. Yuan, M. V. Jiménez, E. Sola, F. J. Lahoz and L. A. Oro, *J. Am. Chem. Soc.*, 2002, **124**, 752; (*c*) R. C. Matthews, D. K. Howell, W.-J. Peng, S. G. Train, W. D. Treleaven and G. G. Stanley, *Angew. Chem., Int. Ed. Engl.*, 1996, **35**, 2253; (*d*) M. E. Broussard, B. Juma, S. G. Train, W. Peng, S. A. Laneman and G. G. Stanley, *Science*, 1993, **260**, 1784; (*e*) J. R. Torkelson, F. H. Antwi-Nsiah, R. McDonald, M. Cowie, J. G. Pruis, K.-J. Jalkanen and R. L. DeKock, *J. Am. Chem. Soc.*, 1999, **121**, 3666; (*f*) J. R. Torkelson, R. McDonald and M. Cowie, *J. Am. Chem. Soc.*, 1998, **120**, 4047; (*g*) M. M. Dell'Anna, S. J. Trepanier, R. McDonald and M. Cowie, *Organometallics*, 2001, **20**, 88; (*h*) Y. Ohki and H. Suzuki, *Angew. Chem., Int. Ed.*, 2000, **39**, 3463; (*i*) T. Shima and H. Suzuki, *Organometallics*, 2000, **19**, 2420; (*j*) K. Tada, M. Oishi and H. Suzuki, *Organometallics*, 1996, **15**, 2422; (*k*) M. D. Fryzuk, S. A. Johnson, B. O. Patrick, A. Albinati, S. A. Mason and T. F. Koetzle, *J. Am. Chem. Soc.*, 2001, **123**, 3960.

6 T. A. Hanna, A. M. Baranger and R. G. Bergman, *J. Am. Chem. Soc.*, 1995, **117**, 11363.

7 (*a*) Y. Gao, J. Kuncheria, G. P. A. Yap and R. J. Puddephatt, *Chem. Commun.*, 1998, 2365; (*b*) Y. Gao, J. K. Kuncheria, H. A. Jenkins, R. J. Puddephatt and G. P. A. Yap, *J. Chem. Soc., Dalton Trans.*, 2000, 3212.

8 (*a*) H. Matsuzaka, K. Ichikawa, T. Ishii, M. Kondo and S. Kitagana, *Chem. Lett.*, 1998, 1175; (*b*) L. Carlton, W. E. Lindsell, K. J. McCullough and P. N. Preston, *J. Chem. Soc., Chem. Commun.*, 1982, 1001; (*c*) C. P. Casey, Y. Wang, R. S. Tanke, P. N. Hazin and E. W. Rutter, Jr., *New J. Chem.*, 1994, **18**, 43; (*d*) D. M. Antonelli and M. Cowie, *Organometallics*, 1990, **9**, 1818.

9 C. P. Casey, R. M. Bullock and F. Nief, *J. Am. Chem. Soc.*, 1983, **105**, 7574.

10 (*a*) B. Chaudret, F. Dahan and S. Sabo, *Organometallics*, 1985, **4**, 1490; (*b*) H. B. Laarab, B. Chaudret, F. Dahan, J. Devillers, R. Poiblanc and S. Sabo-Etienne, *New J. Chem.*, 1990, **14**, 321.

11 O. Oke, R. McDonald and M. Cowie, *Organometallics*, 1999, **18**, 1629.

12 A. Blagg, R. Robson, B. L. Shaw and M. Thornton-Pett, *J. Chem. Soc., Dalton Trans.*, 1987, 2171.

13 S. Ali, A. J. Carty, A. J. Deeming, G. D. Enright and G. Hogarth, *Chem. Commun.*, 2000, 123.

14 C. P. Casey, R. E. Palermo and R. F. Jordan, *J. Am. Chem. Soc.*, 1985, **107**, 4597.

15 R. McDonald and M. Cowie, *Inorg. Chem.*, 1990, **29**, 1564.

16 A. L. Sargent and M. B. Hall, *J. Am. Chem. Soc.*, 1989, **111**, 1563.

17 (*a*) G. Jia and R. H. Morris, *J. Am. Chem. Soc.*, 1991, **113**, 875; (*b*) G. Jia, A. J. Lough and R. H. Morris, *Organometallics*, 1992, **11**, 161.

18 C. P. Kubiak, C. Woodcock and R. Eisenberg, *Inorg. Chem.*, 1982, **21**, 2119.

19 E. Sola, F. Torres, V. Jiménez, J. A. López, S. E. Ruiz, F. J. Lahoz, A. Elduque and L. A. Oro, *J. Am. Chem. Soc.*, 2001, **123**, 11925.

20 R. M. Bullock, J.-S. Song and D. J. Szalda, *Organometallics*, 1996, **15**, 2504.

21 R. M. Bullock and M. H. Voges, *J. Am. Chem. Soc.*, 2000, **122**, 12594.

22 J. S. Field, R. J. Haines, E. Minshall, C. N. Sampson, J. Sundermeyer and S. F. Woollam, *J. Chem. Soc., Dalton Trans.*, 1992, 2629.

23 (*a*) K. Siegmann, P. S. Pregosin and L. M. Venanzi, *Organometallics*, 1989, **8**, 2659; (*b*) M. Meister, J. T. Vandeberg, F. P. Cassaretto, H. Posvic and C. E. Moore, *Anal. Chim. Acta*, 1970, **49**, 481.

24 Bullock and co-workers have pointed out that the group 8 hydrides such as $Cp^*Ru(CO)_2H$ exhibits much greater kinetic hydridicity than the group 6 hydrides $Cp^*Mo(CO)_3H$ and $Cp^*W(CO)_3H$.[25] It is therefore reasonable to assume that the kinetic hydridicity of $Cp'Ru(PR_3)(CO)H$ (Cp' = Cp or Cp*) would also be greater than that of $Cp'M(PR_3)(CO)_2H$ (M = Mo, W).

25 (*a*) T.-Y Cheng and R. M. Bullock, *Organometallics*, 2002, **21**, 2325; (*b*) T.-Y. Cheng, B. S. Brunchwig and R. M. Bullock, *J. Am. Chem. Soc.*, 1998, **120**, 13121.

26 The pK_a of $CpRu(CO)_2H$ is 5 and 6 units higher than those of $CpW(CO)_3H$ and $CpMo(CO)_3H$, respectively.[27] Although the pK_a values of the phosphine-substituted ruthenium hydrides $Cp'Ru(PR_3)(CO)H$ (Cp' = Cp or Cp*) are not available, it is expected that their thermodynamic acidity are substantially lower than that of $Cp'M(PR_3)(CO)_2H$ (M = Mo, W).

27 (*a*) E. J. Moore, J. M. Sullivan and J. R. Norton, *J. Am. Chem. Soc.*, 1986, **108**, 2257; (*b*) S. S. Kristjánsdóttir, J. R. Norton, in *Transition Metal Hydrides*, ed. A. Dedieu, VCH, New York, 1992, ch. 9.

28 (*a*) M. I. Bruce, C. Hameister, A. G. Swincer and R. C. Wallis, *Inorg. Synth.*, 1982, **21**, 78; (*b*) R. B. King and F. G. A. Stone, *Inorg. Synth.*, 1963, **7**, 99.

29 D. P. Tate, W. R. Knipple and J. M. Augl, *Inorg. Chem.*, 1962, **1**, 433.